The Astrophysical Journal, 646:184–191, 2006 July 20

COSMOLOGICAL IMPLICATIONS OF DWARF SPHEROIDAL CHEMICAL EVOLUTION

Yeshe Fenner
Harvard-Smithsonian Center for Astrophysics, 60 Garden Street, Cambridge, MA 02138; yfenner@cfa.harvard.edu

Brad K. Gibson
Centre for Astrophysics, University of Central Lancashire, Preston PR1 2HE, UK; bkgibson@uclan.ac.uk

Roberto Gallino
Dipartimento di Fisica Generale, Universita di Torino, 10125 Torino, Italy; gallino@ph.unito.it

and

Maria Lugaro
Astronomical Institute, University of Utrecht, Postbus 80000, 3508 TA Utrecht, Netherlands; M.Lugaro@phys.uu.nl
Received 2006 February 21; accepted 2006 March 30

ABSTRACT

The chemical properties of dwarf spheroidals in the local group are shown to be inconsistent with star formation being truncated after the reionization epoch ($z \sim 8$). Enhanced levels of [Ba/Y] in stars in dwarf spheroidals like Sculptor indicate strong *s*-process production from low-mass stars whose lifetimes are comparable with the duration of the pre-reionization epoch. The chemical evolution of Sculptor is followed using a model with SN II and SN Ia feedback and mass- and metallicity-dependent nucleosynthetic yields for elements from H to Pb. We are unable to reproduce the Ba/Y ratio unless stars formed over an interval long enough for the low-mass stars to pollute the interstellar medium with *s*-elements. This robust result challenges the suggestion that most of the local group dwarf spheroidals are fossils of reionization and supports the case for large initial dark matter halos.

Subject headings: galaxies: abundances — galaxies: dwarf — galaxies: evolution — Local Group — nuclear reactions, nucleosynthesis, abundances — stars: abundances — stars: AGB and post-AGB

Online material: color figures

1. INTRODUCTION

Dwarf galaxies in the Local Group provide a nearby laboratory for testing dark matter (DM) structure formation scenarios and indirectly probing the epoch of reionization. Many properties of the Milky Way's dwarf spheroidal (dSph) satellites have been well studied, yet their role in the cosmological context is still uncertain. Cosmological simulations have long been plagued by the "missing satellites" problem—the overprediction by up to 2 orders of magnitude of the abundance of DM subhalos with mass $\lesssim 10^8\ M_\odot$ in systems like our Local Group (Klypin et al. 1999). The two most popular explanations for the observed deficit of low-mass satellites are that (1) only massive ($\gtrsim 10^9\ M_\odot$) satellites were able to form stars, with the spheroidal morphology and small present-day stellar velocities of dSphs arising through tidal interactions (e.g., Kravtsov et al. 2004; Kazantzidis et al. 2004), or (2) low-mass satellites ($\lesssim 10^8\ M_\odot$) could form stars but only prior to the reionization epoch, after which UV heating photoevaporates the gas and curtails star formation (Barkana & Loeb 1999; Bullock et al. 2000; Ricotti & Gnedin 2005; Gnedin & Kravtsov 2006). These two solutions have very different, and testable, consequences for the dSph population. The first scenario implies that Galactic dSphs descended from far more massive DM halos than one infers, assuming that mass follows light (i.e., 10^7–$10^8\ M_\odot$; Mateo 1998), while the second scenario implies that many dSphs are very ancient ($z \gtrsim 8$) and associated with less massive DM halos.

Recent work from Ricotti & Gnedin (2005) favors the second scenario, in which most dSphs are "fossils" of reionization. They suggest that internal ionizing sources and, to a lesser extent, UV background radiation prevented the gas from cooling and collapsing to form stars after the reionization era. In this case, almost all star formation (SF) activity transpired in an interval of $\lesssim 600$ Myr.[1] This relatively brief window of opportunity for SF should leave observable signatures on the stellar chemical properties. A commonly used "clock" of SF is α/Fe versus metallicity (Matteucci & Recchi 2001). This is because α-elements like O, Mg, and Si are generated primarily in short-lived massive stars culminating as Type II supernovae (SNe II), whereas a substantial fraction of Galactic Fe is attributed to Type Ia SNe (SNe Ia), which occur on longer timescales (Timmes et al. 1995). The first generation of SNe II pollute their host galaxy with supersolar α/Fe gas, while a delayed contribution from SNe Ia subsequently leads to a decrease in α/Fe with increasing Fe/H. Thus, a system with low α/Fe at low metallicity is interpreted as having undergone slow and protracted SF, whereas stars born in a short intense burst should exhibit higher α/Fe. Unfortunately, α/Fe does not uniquely trace SF. Dwarf galaxies are especially vulnerable to feedback effects that may foster the preferential loss of elements from massive SNe II, thus complicating the interpretation of the α/Fe diagnostic.

In this paper we employ the abundance pattern of neutron-capture elements, particularly those associated with the slow neutron-capture process (known as the *s*-process), as a better chemical test of SF duration in dSphs. Venn et al. (2004) suggested that the overabundance of [Ba/Y] in most dSphs was consistent with the production of *s*-elements from lower mass stars. We confirm that the curious behavior of the relative abundance of

[1] Here we have assumed ΛCDM cosmology with present-day $\Omega_m = 0.34$, $\Omega_\Lambda = 0.66$, Hubble parameter = 70 km s^{-1} Mpc^{-1}, and a 13 Gyr age for the universe.

neutron-capture elements Y, Ba, and Eu in dSphs reflects a strong contribution from low-mass stars, which are the chief source of the *s*-elements (Busso et al. 1999). Owing to the correspondingly long lifetimes of these low-mass stars, one can use chemical evolution simulations to place limits on the minimum duration of star formation allowed by the observations. In § 2 we give the details of our chemical evolution model of the representative dwarf galaxy Sculptor. Section 3 presents results from models with different star formation histories, in order to assess whether dSphs are survivors or fossils of the epoch of reionization, and § 4 contains our main conclusions.

2. THE MODEL

We have modeled the chemical evolution of the dwarf spheroidal Sculptor on the assumption that its evolution and SF history is typical of the types of dSph galaxies that Ricotti & Gnedin (2005) identified as likely fossils of reionization. Moreover, its proximity makes Sculptor one of the best-studied dSphs with a large set of chemical abundance constraints (e.g., Shetrone et al. 2003; Geisler et al. 2005). This section summarizes the key features of the model, which is described in greater detail in Y. Fenner et al. (2006, in preparation), where it is applied to 10 local group dwarf spheroidals and irregulars.

2.1. *Equations*

The chemical enrichment history of Sculptor was simulated using a modified version of the chemical evolution code described in Fenner & Gibson (2003) and Fenner et al. (2003, 2004). Major changes made to the code include allowing for SN-driven outflows, employing the star formation history from Dolphin et al. (2005), and adding s- and *r*-process yields. The evolution of the gas phase abundance pattern reflects the cumulative history of the dynamic processes of star formation, gas inflows and outflows, stellar evolution, and nucleosynthesis. The set of equations governing these processes were numerically solved by defining $\sigma_i(t)$ as the mass surface density of species i at time t, and assuming that the rate of change of $\sigma_i(t)$ is given by

$$\frac{d}{dt}\sigma_i(t) = E_{i,\mathrm{LIMS}}(t) + E_{i,\mathrm{SN\,II}}(t) + E_{i,\mathrm{SN\,Ia}}(t) - W_{i,\mathrm{ISM}}(t) - W_{i,\mathrm{SN\,II}}(t) - W_{i,\mathrm{SN\,Ia}}(t) + \frac{d}{dt}\sigma_i(t)_{\mathrm{infall}} - X_i(t)\psi(t), \quad (1)$$

where the first three terms, $E_{i,\mathrm{LIMS}}(t)$, $E_{i,\mathrm{SN\,II}}(t)$, and $E_{i,\mathrm{SN\,Ia}}(t)$, denote the mass surface density of species i ejected at time t by low- and intermediate-mass stars (LIMSs), SNe II and SNe Ia, respectively. The following term, $W_{i,\mathrm{ISM}}(t)$, denotes the mass surface density of species i that escapes from the neutral galactic interstellar medium (ISM) due to being carried along with SN-driven winds. The next two terms, $W_{i,\mathrm{SN\,II}}(t)$ and $W_{i,\mathrm{SN\,Ia}}(t)$, represent mass of species i released by SNe II and SNe Ia, respectively, that is expelled via winds. The term $(d/dt)\sigma_i(t)_{\mathrm{infall}}$ gives the infall rate of i, which is determined by calculating the amount of gas required to ensure that the star formation rate (SFR) satisfies the Kennicutt law (see § 2.2). The chemical composition of the infalling gas (and the gas at the first time step) was taken to be primordial. The final term, $X_i(t)\psi(t)$, gives the depletion of species i due to incorporation into newly formed stars, where $X_i(t)$ is the mass fraction of i in the ISM at time t and $\psi(t)$ is the SFR. The ejection rates in equation (1), specifying the production of each element from the different types of star, are given by

$$E_{i,\mathrm{LIMS}}(t) = \int_{m_{\mathrm{low}}}^{m_{\mathrm{bl}}} \psi(t-\tau_m) Y_i(m,\ Z(t-\tau_m)) \frac{\phi(m)}{m}\, dm + (1-A)\int_{m_{\mathrm{bl}}}^{m_{\mathrm{bu}}} \psi(t-\tau_m) \times Y_i(m,\ Z(t-\tau_m)) \frac{\phi(m)}{m}\, dm, \quad (2)$$

$$E_{i,\mathrm{SN\,Ia}}(t) = A\int_{m_{\mathrm{bl}}}^{m_{\mathrm{bu}}} \frac{\phi(m_b)}{m} \times \left[\int_{\mu_m}^{0.5} f(\mu)\psi(t-\tau_{m_2}) \times Y_{b,i}(m,\ Z(t-\tau_{m_2}))d\mu\right] dm_b, \quad (3)$$

$$E_{i,\mathrm{SN\,II}}(t) = \int_{m_{\mathrm{bu}}}^{m_{\mathrm{up}}} \psi(t-\tau_m) \times Y_i(m,\ Z(t-\tau_m)) \frac{\phi(m)}{m}\ dm, \quad (4)$$

where $Y_i(m,\ Z(t-\tau_m))$ is the stellar yield of i (in mass units) from a star of mass m, main-sequence lifetime τ_m, and metallicity $Z(t-\tau_m)$. The initial mass function, $\phi(m)$, has upper and lower mass limits of $m_{\mathrm{up}} = 60$ and $m_{\mathrm{low}} = 0.08\ M_\odot$, respectively. The models presented here employ the Kroupa et al. (1993) three-component IMF. The fraction of LIMS in binary systems culminating in a SN Ia is given by parameter A. The SN Ia progenitor binary mass is denoted by m_b and is the sum of the primary and secondary masses, $m_1 + m_2$. The binary mass has upper and lower limits of $m_{\mathrm{bu}} = 16$ and $m_{\mathrm{bl}} = 3\ M_\odot$, respectively. The function $f(\mu)$ determines the distribution for the mass fraction of the secondary ($\mu = m_2/m_b$). The reader is referred to Matteucci & Greggio (1986) for more detailed discussion and definitions of the terms in the above equations.

Most previous studies (e.g., Lanfranchi & Matteucci 2003, 2004; Lanfranchi et al. 2006; Robertson et al. 2005) have assumed differential galactic winds in proportion to the SFR. These have assumed $W_i(t) = w_i\psi(t)$, where w_i is a free parameter that is arbitrarily set for each element in order to reproduce observations and is then kept constant as a function of time. Such a scheme does not allow for behavior such as increased escape of Fe relative to O after a burst of SF when the frequency of SNe Ia may compare with, or exceed, that of SNe II. Instead, we self-consistently calculate the amount of SN II and SN Ia ejecta lost at each time step as a function of the appropriate SN rates. Cold interstellar gas also escapes from the galaxy by imposing a mass-loading factor that is consistent with observations. The form of the equations governing the loss of species i in galactic winds can be written

$$W_{i,\mathrm{SN\,Ia}}(t) = E_{i,\mathrm{SN\,Ia}}(t)\min\left(0.9,\ \frac{\epsilon_{\mathrm{SN\,Ia}}}{m_{\mathrm{tot}}}R_{\mathrm{SN\,Ia}}\right), \quad (5)$$

$$W_{i,\mathrm{SN\,II}}(t) = E_{i,\mathrm{SN\,II}}(t)\min\left(0.9,\ \frac{\epsilon_{\mathrm{SN\,II}}}{m_{\mathrm{tot}}}R_{\mathrm{SN\,II}}\right), \quad (6)$$

$$W_{i,\mathrm{ISM}}(t) = X_i(t)\mathrm{ML}[W_{\mathrm{gas,SN\,Ia}}(t) + W_{\mathrm{gas,SN\,II}}(t)], \quad (7)$$

where m_{tot} is the total galaxy mass in units of $10^6\ M_\odot$ (taken from Mateo 1998). The SN Ia and II rates are given by $R_{\mathrm{SN\,Ia}}$ and

$R_{\rm SN\ II}$, while the corresponding wind efficiency factors are $\epsilon_{\rm SN\ Ia}$ and $\epsilon_{\rm SN\ II}$. The mass of element i in the ISM that gets entrained in the SN-driven winds and driven out of the galaxy is set by the mass-loading factor, ML (=15, as discussed below). The sum of $W_{\rm gas,SN\ Ia}(t)$ and $W_{\rm gas,SN\ II}(t)$ gives the total amount of stellar ejecta lost in winds at time t and is equivalent to the sum of $W_{i,\rm SN\ Ia}(t)$ and $W_{i,\rm SN\ II}(t)$ over all i. The escape fraction of SN II and SN Ia ejecta increases linearly with their respective SN rates, but the overall efficiency is inversely proportional to the depth of the galactic potential well, as measured by the total galaxy mass, $m_{\rm tot}$. We do not allow more than 90% of the SN ejecta to escape at each time step, on the basis of the prediction by Hensler et al. (2004) that up to 25% of SN material gets mixed into the local ISM on short timescales rather than being carried away by an expanding superbubble. We note that the main conclusions of this paper are robust to the implementation of feedback.

Martin et al. (2002) estimated that the diffuse halo gas of the dwarf starburst NGC 1569 has α/Fe $\sim$ 2–4 times solar. The metallicity of the hot halo gas was measured to be roughly solar, implying a mass-loading factor of $\sim$9. In order to obtain [O/Fe] $\sim$ +0.3 to +0.6 in the galactic winds, we assume that SNe Ia and SNe II have the same explosion energy of 10^{51} ergs and we set the feedback efficiency for SNe Ia to be 5 times higher than that of SNe II. This might seem counterintuitive, given that SNe II occur in associations, which should enhance their ability to heat the ISM and create bubbles and chimneys facilitating the escape of metals. However, Recchi et al. (2004, 2006) argue that SNe II are *less* efficient at expelling their ejecta, because much of their energy goes toward heating the cold dense molecular clouds from which they were born. The characteristic lifetimes of SNe Ia range from tens to thousands of Myr, by which time the SN Ia progenitors will have traveled to regions of lower density, where less energy is required to widely disperse ejecta.

We assume that turbulent motions at the boundary between the SN-driven winds and the ambient ISM mix significant quantities of cold gas into the outflows. Our adopted mass-loading factor of 15 is similar to the value inferred for NGC 1569 and the value of 10 calculated by Silk (2003). The mass-loading factor (i.e., the mass of the ISM carried away with the winds relative to the mass of stellar ejecta in the wind) is the key parameter determining the metallicity of the galactic outflows.

Observations of superwinds in starburst galaxies by Heckman et al. (2000) reveal outflow rates (OFRs) comparable with the SFR. Theoretical calculations support this approximate equivalence between the OFR and SFR (Silk 2003; Shu et al. 2005). Silk (2003) estimated that OFR is similar to SFR in the case of large porosity, and OFR is less than SFR when porosity is low. Accordingly, our overall wind efficiency was chosen to produce outflow rates roughly half the SFR. We also assumed that galactic wind efficiency is inversely proportional to the total galaxy mass, where galaxy mass was taken from Mateo (1998).

Given a velocity dispersion of about 2 km s^{-1} for stars in OB associations (Tian et al. 1996) and lifetimes >60 Myr for low- and intermediate-mass stars (Schaller et al. 1992), then most LIMS will have drifted outside the $\sim$50–100 pc radii of the stellar association in which they were born by the time they begin to pollute the ISM with their winds. Owing to their weak stellar winds and their likely migration from OB bubbles, we mix the newly released ejecta from LIMS directly into the ISM at each time step.

2.2. *Star Formation History* (*SFH*)

We tested two different star formation histories: (1) model A adopts the SF history inferred from Sculptor's color-magnitude diagram (Dolphin et al. 2005) in which SF extends for over several Gyr and (2) model B compresses the SF within a period of 600 Myr. Figure 1 compares these two SF histories. The gas accretion rate is often treated as an input into chemical evolution models; however, we work backward to infer the infall rates from the SFHs by inverting the Kennicutt (1998) SF law. Like Lanfranchi & Matteucci (2003, 2004; Lanfranchi et al. 2006), we find that low SF efficiencies are better able to reproduce the chemical abundances in local group dwarf galaxies. In particular, we obtain good fits in our standard model using $\psi(t) = 0.05\sigma(t)^{1.4}\ M_\odot\ {\rm pc}^{-2}\ {\rm Gyr}^{-1}$, where ψ is the SFR and σ is the gas surface density. The difference between the $\sigma(t)$ implied by the $\psi(t)$ and the value predicted within the chemical evolution models provides the infall rate at each time step.

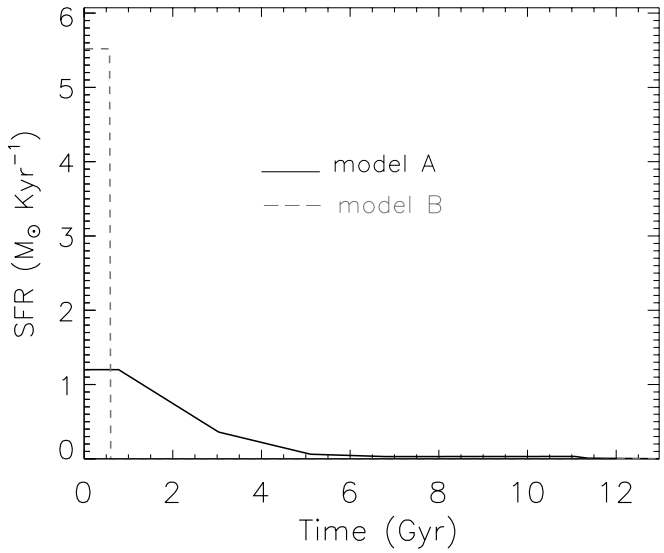

FIG. 1.—Star formation rate in units of $M_\odot$ per thousand years as a function of time for models A and B. [*See the electronic edition of the Journal for a color version of this figure.*]

2.3. *Stellar Yields*

2.3.1. *Low- and Intermediate-Mass Stars*

For the production of isotopes up to the Fe peak from stars less massive than 8 $M_\odot$, we incorporated yields from the stellar evolution and nucleosynthesis code described in Karakas & Lattanzio (2003), supplemented with unpublished yields for the metallicity $Z = 0.0001$. The origin and interpretation of *s*-process elements like La, Ba, and Y in the local group is of considerable import to this study. The Karakas et al. models do not calculate the *s*-process, so for elements above the Fe-peak, we employ the nucleosynthetic yields of the Torino group (R. Gallino et al. 2006, in preparation). These mass- and metallicity-dependent yields have previously been used in the Galactic chemical evolution models of Travaglio et al. (1999, 2001, 2004). In a similar fashion to Travaglio et al., we have averaged the *s*-process yields over a range of ^{13}C pocket choices.

The slow neutron-capture process in asymptotic giant branch (AGB) stars is thought to be driven primarily by the $^{13}{\rm C}(\alpha,\ n)^{16}{\rm O}$ reaction, which provides the flux of neutrons that can be captured by elements from the Fe-peak upward (Busso et al. 1999). The source of the ^{13}C probably comes from CN-cycling in the H envelope leading to proton capture by ^{12}C and the development of a pocket of ^{13}C at the top of the intershell region between the H shell and He shell. This pocket arises through the diffusion of a small amount of protons from the H envelope at the epoch of the third dredge-up episodes. Proton mixing is induced by the close

contact between the convective H-rich envelope and the radiative He-rich and C-rich He intershell, thus forming a tiny "proton pocket." These protons are subsequently captured by the abundant ^{12}C in the He intershell, creating a ^{13}C pocket of primary nature. Afterward, when the pocket is heated up to about 0.9×10^8 K, ^{13}C is consumed by α captures that release neutrons and give rise to a very intense neutron exposure. The formation of the ^{13}C pocket is not simulated within the nucleosynthesis codes but rather is treated parametrically and constrained by observations (Busso et al. 1999).

2.3.2. *Type Ia Supernovae*

We adopted a recalculation of the Thielemann et al. (1986) W7 model by Iwamoto et al. (1999) to estimate the yields from SNe Ia. It was assumed that 4% of binary systems involving intermediate- and low-mass stars result in SNe Ia, since this fraction provides a good fit to the solar neighborhood (e.g., Alibés et al. 2001; Fenner & Gibson 2003).

2.3.3. *Massive Stars*

For stars more massive than 8–10 $M_\odot$ that end their lives in violent supernova explosions, we implemented the yields from Woosley & Weaver (1995) for elements up to Zn (using the same technique as in Fenner et al. [2003, 2004], and halving the Fe yield, as suggested by Timmes et al. [1995]). Beyond Zn, the yields of *r*-process elements like Eu are difficult to calculate within nucleosynthesis models, and it is common practice to assume primary production from SNe II and empirically deduce them (e.g., Argast et al. 2004) or estimate them by calculating the difference between the solar abundance and the pure *s*-process contribution predicted by Galactic chemical evolution models (e.g., Travaglio et al. 1999, 2001, 2004). Although the stellar mass range responsible for *r*-production is still under debate (e.g., Sumiyoshi et al. 2001; Wanajo et al. 2003; Tsujimoto et al. 2000), our models link the *r*-process site to all SNe II with mass $<40\ M_\odot$. We tested the case in which only SNe II with mass $<15\ M_\odot$ produced *r*-elements, finding that the conclusions of this paper are not very sensitive to the adopted mass range. Metallicity-dependent main-sequence lifetimes calculated by Schaller et al. (1992) have been employed.

3. RESULTS

Figure 2 shows the predicted abundances of O, Mg, Si, Ca, Sc, and Ti relative to Fe from the Sculptor model using (1) the standard SFH inferred from observations (model A: *solid contour lines and shaded region*) and (2) the suppressed SF model (model B: *dashed contour lines*). To illustrate the role of feedback and preferential loss of SN ejecta, we also show results from an identical simulation to model A but *without* galactic winds (model C: *dotted contour lines*). Red giant stars observed in Sculptor by Shetrone et al. (2003) and Geisler et al. (2005) (*diamonds*) have a mean $[\mathrm{Fe/H}] \sim -1.57$, which is well matched by our predicted mean of $[\mathrm{Fe/H}] \sim -1.65$. We also produce a metallicity spread in agreement with the data. Sculptor stars exhibit α/Fe ratios[2] slightly above solar at the lowest metallicities, before declining to subsolar values at higher [Fe/H] ($\gtrsim -1.5$). Note that the subsolar [α/Fe] values in Sculptor stars contrasts dramatically with the supersolar ratios characterizing MW stars at the same metallicity. This is thought to be common in dwarf galaxies whose low gas surface densities lead to inefficient SF and consequently long metal enrichment timescales. However, we find that subsolar α/Fe can arise through the preferential loss of SN products via galactic winds (cf. models A and C). Both the standard and suppressed SF models satisfactorily reproduce the overall α-element trends. The standard SF model has slightly lower (by ~ 0.1 dex) O, Si, Ca, Sc, and Ti with respect to Fe than in the suppressed SF model, but the influence of galactic winds makes the difference smaller than for a closed box model. The prevention of SN feedback (*dotted contour lines*) leads to an excess of O, Si, and Ca, in conflict with the data. Figure 2 demonstrates that [α/Fe] is not a clean probe of SF history in galaxies that have experienced metal-enriched outflows. Indeed, [α/Fe] is more sensitive in our Sculptor models to SN feedback than to the duration of SF.

Conversely, Figure 3 suggests that the neutron-capture elements provide a more useful discriminant of the different star formation models. The neutron-capture elements show curious patterns in Sculptor stars (e.g., Venn et al. 2004). The light *s*-process element Y tends to be subsolar relative to Fe, and lower than that in Milky Way stars of comparable metallicity. Conversely, the heavy *s*-process element Ba is slightly higher than in Galactic field stars. In our models, the Sculptor stars with enhanced Ba/Y ratios were born from gas that had been heavily polluted by low-mass stars. The high [Ba/Y] ratio can only be matched by our model incorporating both SN-driven winds and SF extending over several Gyr. This is because the origin of gas with $[\mathrm{Ba/Y}] \gtrsim +0.5$ dex is low-mass metal-poor stars on the AGB, whose weak ($\sim$15–30 km s^{-1}) winds are easily retained by the potential well.

For low-mass AGB stars to dominate *s*-element abundances in the ISM there needs to be substantial loss of SN II ejecta *and* SF timescales exceeding the lifetimes of low-mass stars. The strong metallicity dependence of *s*-process yields from AGBs gives rise to the sharp upturn in Ba and La abundance at $[\mathrm{Fe/H}] \sim -1.6$. This leads to some stars having Ba enhancements as high as that observed, although the fraction of simulated stars with supersolar Ba relative to Fe, Y, and Eu is underestimated, even in model A. This may inform us about the size and nature of the ^{13}C pocket in metal-poor AGB stars. AGB stars produce heavier *s*-elements like La and Ba more efficiently than lighter species like Y at low metallicities. This is because the neutron flux per seed nuclei varies roughly inversely with metallicity. Since the slow neutron-capture process proceeds further along the periodic table with decreasing initial stellar metallicity, Pb production from AGBs peaks at lower [Fe/H], followed by a Ba and La peak at higher [Fe/H]. The production of Y from AGBs reaches peak efficiency at higher [Fe/H] than is typical for dSphs. A further prediction from our model is that dwarf spheroidal stars should have supersolar [Pb/Ba] and [Pb/Fe] ratios. Although Pb requires a very high signal-to-noise ratio and has not yet been measured in stars outside the Milky Way, sufficient exposure time may yield future detections in red giants in nearby dSphs. Such measurements would be a very useful test of this model and may provide insight into the nature of the *s*-process in low-mass stars.

The relative importance of the *s*- and *r*-processes is usually measured by the [Ba/Eu] ratio, where the pure *r*-process ratio is $[\mathrm{Ba/Eu}] \sim -0.8$ dex and the pure *s*-process ratio is $\sim$+1 dex (Arlandini et al. 1999). Figure 3 shows about an order of magnitude rise in Ba/Eu going from [Fe/H] = -2 to -1. Sculptor stars tend toward [Ba/Eu] = +0.5 at [Fe/H] = -1, which is 0.8 dex above the corresponding MW value. Only model A reproduces this trend, owing to the retention of lower mass stellar ejecta and the preferential loss of the ejecta from SNe II, which are major suppliers of Eu. The good agreement between model A predictions and the observed [Ba/Fe], [La/Fe], and [Ba/Eu]

[2] The α-elements include O, Mg, Si, Ca, and Ti. Although we also plot Sc in this figure, it is classed as an iron-peak element.

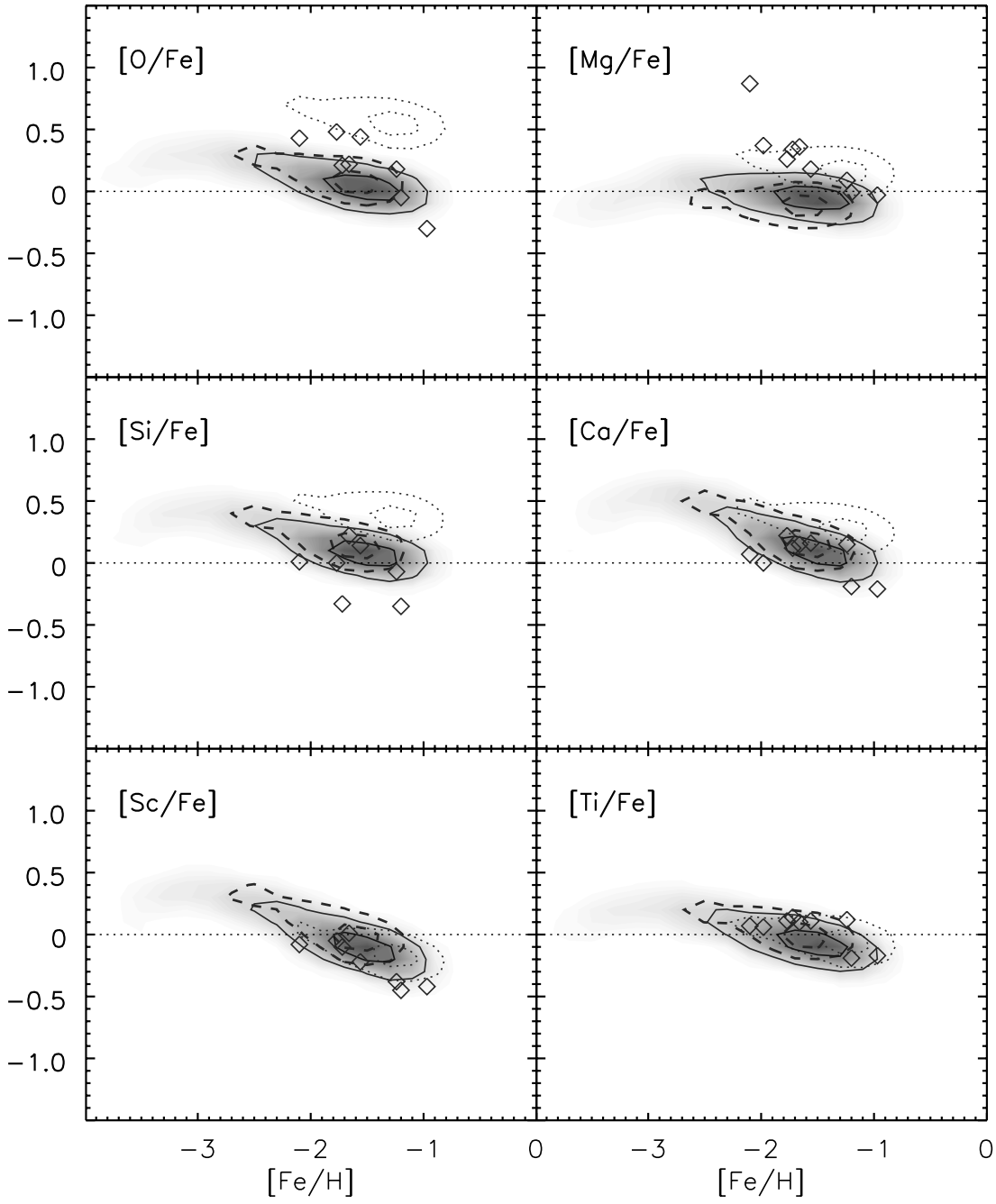

FIG. 2.—Predicted abundances for the Sculptor dSph chemical evolution model, incorporating SN feedback and galactic winds, plotted against stellar observations from Shetrone et al. (2003) and Geisler et al. (2005; *diamonds*). The shaded region indicates the relative frequency of stars from model A as a function of [X/Y] and [Fe/H], where [X/Y] is indicated in the top left-hand corner of each panel. Pairs of contour lines are plotted at 0.25 and 0.75 of the maximum frequency. The predicted stellar abundances have been convolved with a Gaussian of dispersion 0.1 dex to mimic observational uncertainties. Results from model B, in which SF is shut off by reionization after 0.6 Gyr, are shown by dashed contour lines. Dotted contour lines correspond to model C, which is the same as model A but without SN feedback. [*See the electronic edition of the Journal for a color version of this figure.*]

lends further support to the case for extended SF in dSphs. We place more weight on the Ba/Y diagnostic, however, since there is no obvious alternative to low-mass stars that can match the high values measured.

Interestingly, the massive Galactic globular cluster ω Centauri exhibits similar chemical properties, with the lowest metallicity stars ($[\mathrm{Fe/H}] \sim -1.8$) having a predominantly *r*-process abundance pattern and those with the highest metallicity ($[\mathrm{Fe/H}] \sim -0.8$) having dramatic enhancements in *s*-process elements (Smith et al. 2000). Smith et al. attributed these observations to the greater retention of low-mass stellar ejecta—because of their weak winds—compared with energetic SN II winds. They infer that star formation must have continued for at least several Gyr, making ω Centauri highly anomalous compared with other globular clusters, whose individual stellar populations formed contemporaneously. Indeed, it has been suggested (e.g., Majewski et al. 2000) that ω Centauri is not a globular cluster but rather the remains of an accreted dwarf spheroidal.

To further illustrate the time delay associated with *s*-process enrichment, Figure 4 displays the ratio of [Ba/Y] in the ejecta of AGB stars as a function mass for the three metallicities $[Z/\mathrm{H}] = -1.9, -1.6$, and -1.2 for the standard choice of ^{13}C pocket mass

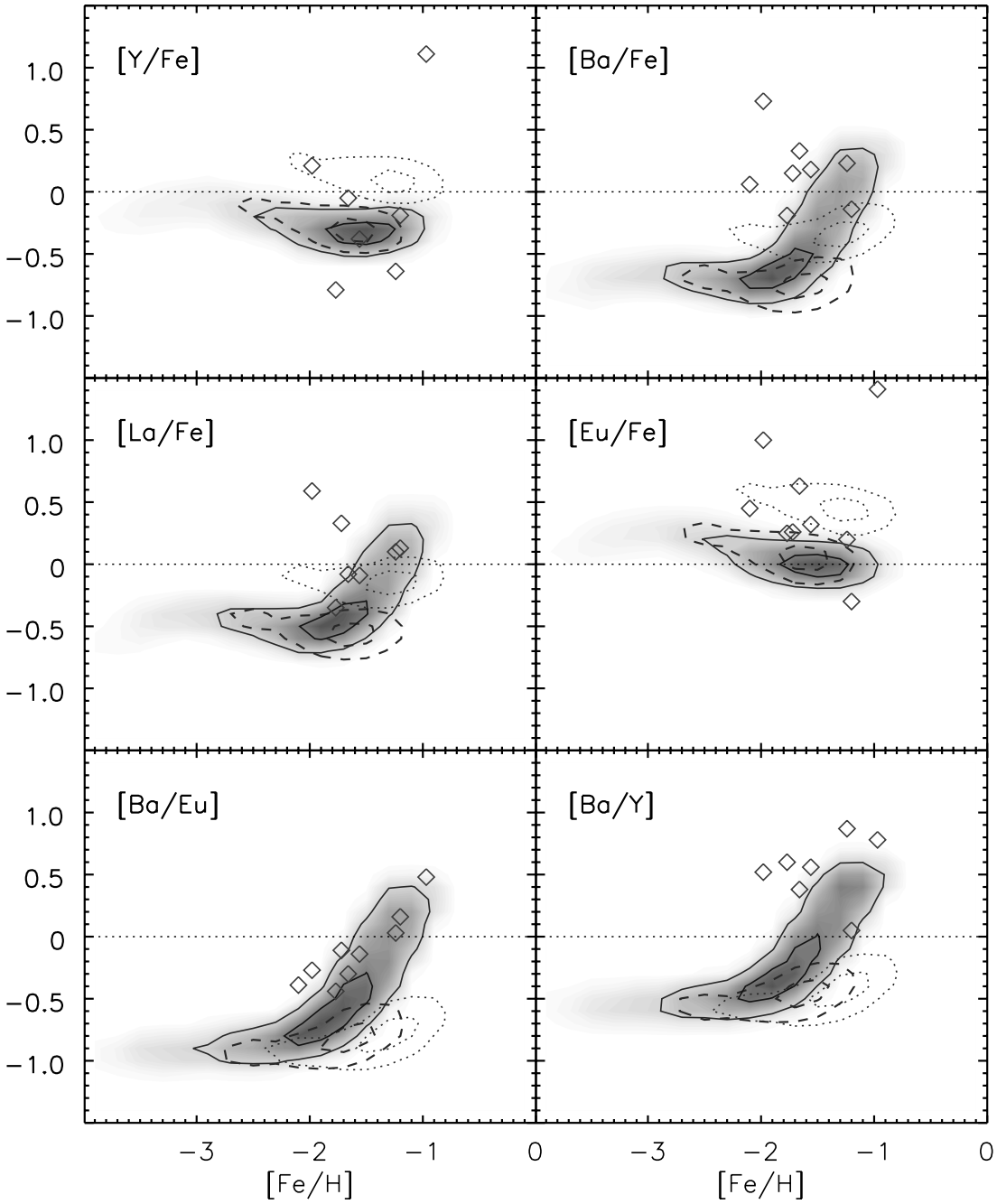

FIG. 3.—Same as Fig. 2, but for neutron-capture elements. The shaded region indicates the relative frequency of stars from model A as a function of [X/Y] and [Fe/H], where [X/Y] is indicated in the top left-hand corner of each panel. Pairs of contour lines are plotted at 0.25 and 0.75 of the maximum frequency. The predicted stellar abundances have been convolved with a Gaussian of dispersion 0.1 dex to mimic observational uncertainties. Results from model B, in which SF is shut off by reionization after 0.6 Gyr, are shown by dashed contour lines. Dotted contour lines correspond to model C. [*See the electronic edition of the Journal for a color version of this figure.*]

(see Travaglio et al. [1999, 2001, 2004] for further details regarding the ^{13}C pocket). The corresponding stellar lifetimes (from Schaller et al. [1992], for a metallicity of $Z = 0.001$) are presented along the top axis. Sculptor stars have a mean $\langle[\mathrm{Fe/H}]\rangle \sim -1.6$ dex and $\langle[\mathrm{Ba/Y}]\rangle \sim 0.5$ dex. From Figure 4 it can be seen that at metallicities typical of dSphs, only AGB stars with mass $\lesssim 3\ M_\odot$ and lifetimes $\gtrsim 300$ Myr have yields with [Ba/Y] $\gtrsim 0.5$ dex. Stars whose yields have [Ba/Y] equal to the highest values measured in Sculptor stars have lifetimes >1 Gyr. If these stars polluted the ISM with Ba-rich gas from which subsequent generations of stars formed, then stars must have been forming for several Gyr or more. We note that with a factor of 1.5 reduction in the ^{13}C pocket, slightly more massive AGB stars can yield [Ba/Y] $\gtrsim$ 0.5 dex on shorter timescales (mass $\lesssim 4\ M_\odot$ and lifetimes $\gtrsim$150 Myr). Indeed, smaller ^{13}C pockets may help resolve the underproduction of [Ba/Y] and [Ba/Fe] seen in Figure 3. After weighting by the IMF, however, lower mass stars dominate the production of *s*-elements and still require extended SF in order to pollute the ISM to the observed levels.

We have argued that the suppression of SF by reionization after ~600 Myr would not grant low-mass stars enough time to pollute the ISM with *s*-elements to the extent demanded by the observations. However, there is still uncertainty regarding the precise redshift at which the universe was reionized. To test

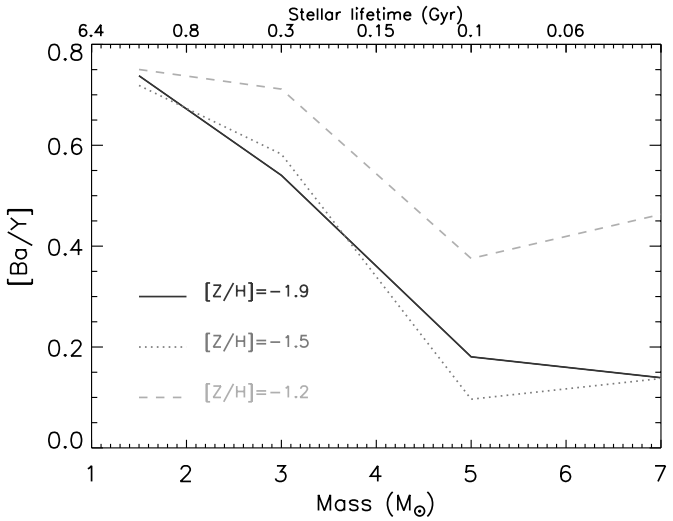

FIG. 4.—[Ba/Y] in the ejecta from AGB stars vs. initial stellar mass for the three metallicities indicated (for a choice of ^{13}C pocket mass of $\sim 4 \times 10^{-6}\ M_{\odot}$) Corresponding stellar lifetimes from Schaller et al. (1992; for $Z = 0.001$) are indicated along the top axis. [*See the electronic edition of the Journal for a color version of this figure.*]

the sensitivity of our results to the assumed redshift of reionization, we ran an identical model with $z_{\rm reion} \sim 6$, which is roughly the lowest value permitted by observations (e.g., Benson et al. 2006; Fan et al. 2006). This model generously allowed SF to continue for 0.9 Gyr, yet the mean [Ba/Y] and [Ba/Eu] increased by less than 0.15 dex and still violated the empirical constraints.

Grebel & Gallagher (2004) found little evidence for reionization suppressing local group galaxy evolution, on the basis of (1) metallicity spreads, (2) low [α/Fe] ratios, and (3) stellar ages. However, a range in metallicites along with low [α/Fe] can both arise from a short star formation episode (see Fig. 2, *dashed contour lines*). The clearest sign of ongoing SF would be an age spread; however, age-dating old stellar populations is complicated by the age-metallicity degeneracy and is subject to uncertainties $\gtrsim$1 Gyr (e.g., Hernandez et al. 2000).Using *s*-element enrichment from long-lived low-mass stars as an alternative chronometer, we arrive at the same conclusion as Grebel & Gallagher (2004).

If early reionization was not responsible for shutting off SF in dSphs like Sculptor, what ultimately caused star formation to cease after a few Gyr? In our models, SN feedback can remove the bulk of the *metals* from Sculptor (and the other dSphs, as shown in Y. Fenner et al. 2006, in preparation), but only a small fraction of the ISM gets carried away by the SN-driven winds. Consequently, our Sculptor model has a final gas fraction of $\sim$70%, whereas most dSphs are observed to have gas fractions less than a percent. Lower gas fractions could be obtained by invoking unreasonably strong galactic winds; however, a more likely mechanism for gas removal is via tidal- and ram-pressure stripping when the orbits of the dSphs bring them into close proximity with the Milky Way halo (e.g., Marcolini et al. 2003, 2004, 2006; Mayer et al. 2005).

4. DISCUSSION AND CONCLUSIONS

We find that the abundance of neutron-capture elements in dwarf spheroidal stars is indicative of a strong contribution from long-lived low-mass stars. While this study presented models of Sculptor, our conclusions apply equally to other old gas-poor dSphs like Draco, Ursa Minor, and Sextans, since they also exhibit enhanced Ba/Y and have similar star formation histories to Sculptor (Dolphin et al. 2005). The observed supersolar Ba/Y ratios imply that stars formed over an interval of at least several Gyr to allow time for metal-poor AGB stars to enrich the ISM with *s*-elements. These results cast doubt on recent suggestions that local group dSphs Draco, Ursa Minor, and Sextans are "fossils" of reionization (Ricotti & Gnedin 2005; Gnedin & Kravtsov 2006). Because the Ba/Y ratio is very high in all dSphs for which it has been measured, we propose that all dSphs were actively forming stars beyond the epoch of reionization. This is indirect evidence for their initial dark matter halos being larger than the $\sim 10^7\ M_{\odot}$ values obtained by assuming that mass follows light (Mateo 1998).

The case for large mass-to-light ratios and extended DM halos in dSphs continues to strengthen. Mashchenko et al. (2005) estimated virial masses of $\sim 10^9\ M_{\odot}$ for Draco, Sculptor, and Carina using *N*-body simulations designed to fit the observed stellar density and velocity profiles. Dehnen & King (2006) indirectly infer a DM halo mass $\gtrsim 10^9\ M_{\odot}$ for Sculptor from its large abundance of X-ray binaries, whose high expected velocities should have facilitated their escape if the potential well was smaller. Moreover, there appears to be an absence of tidal heating at large radii in Draco, Ursa Minor, Sextans, and Sculptor, which implies large and extended DM halos (Read et al. 2006; Coleman et al. 2005). The chemical properties of the representative dwarf spheroidal Sculptor are well matched by our simulations incorporating SN-driven feedback and empirical star formation histories. We contend that the neutron-capture abundance pattern reflects enrichment from metal-poor low-mass stars, which is inconsistent with a cessation in star formation after the reionization epoch and instead supports dSphs having large initial DM halos.

Y. F. thanks Brant Robertson, Adam Lidz, and Timothy Beers for valuable conversations and comments. Y. F. acknowledges the support of an ITC fellowship from the Harvard College Observatory. M. L. has been supported by an NWO VENI grant. R. G. acknowledges support by the Italian MIUR-FIRB project "Origin of the heavy elements beyond Fe."

REFERENCES

Alibés, A., Labay, J., & Canal, R. 2001, A&A, 370, 1103
Argast, D., Samland, M., Thielemann, F.-K., & Qian, Y.-Z. 2004, A&A, 416, 997
Arlandini, C., Käppeler, F., Wisshak, K., Gallino, R., Lugaro, M., Busso, M., & Straniero, O. 1999, ApJ, 525, 886
Barkana, R., & Loeb, A. 1999, ApJ, 523, 54
Benson, A. J., Sugiyama, N., Nusser, A., & Lacey, C. G. 2006, MNRAS, in press
Bullock, J. S., Kravtsov, A. V., & Weinberg, D. H. 2000, ApJ, 539, 517
Busso, M., Gallino, R., & Wasserburg, G. J. 1999, ARA&A, 37, 239
Coleman, M. G., Da Costa, G. S., & Bland-Hawthorn, J. 2005, AJ, 130, 1065
Dehnen, W., & King, A. 2006, MNRAS, 367, L29
Dolphin, A. E., Weisz, D. R., Skillman, E. D., & Holtzman, J. A. 2005, preprint (astro-ph/0506430)
Fan, X., et al. 2006, AJ, 132, 117
Fenner, Y., & Gibson, B. K. 2003, Publ. Astron. Soc. Australia, 20, 189
Fenner, Y., Gibson, B. K., Lee, H.-C., Karakas, A. I., Lattanzio, J. C., Chieffi, A., Limongi, M., & Yong, D. 2003, Publ. Astron. Soc. Australia, 20, 340
Fenner, Y., Prochaska, J. X., & Gibson, B. K. 2004, ApJ, 606, 116
Geisler, D., Smith, V. V., Wallerstein, G., Gonzalez, G., & Charbonnel, C. 2005, AJ, 129, 1428
Gnedin, N. Y., & Kravtsov, A. V. 2006, ApJ, submitted (astro-ph/0601401)
Grebel, E. K., & Gallagher, J. S. 2004, ApJ, 610, L89
Heckman, T. M., Lehnert, M. D., Strickland, D. K., & Armus, L. 2000, ApJS, 129, 493
Hensler, G., Köppen, J., Pflamm, J., & Rieschick, A. 2004, in IAU Symp. 217, Recycling Intergalactic and Interstellar Matter, ed. P.-A. Duc, J. Braine, & E. Brinks (San Francisco: ASP), 178

Hernandez, X., Gilmore, G., & Valls-Gabaud, D. 2000, MNRAS, 317, 831
Iwamoto, K., Brachwitz, F., Nomoto, K., Kishimoto, N., Umeda, H., Hix, W. R., & Thielemann, F.-K. 1999, ApJS, 125, 439
Karakas, A. I., & Lattanzio, J. C. 2003, Publ. Astron. Soc. Australia, 20, 279
Kazantzidis, S., Mayer, L., Mastropietro, C., Diemand, J., Stadel, J., & Moore, B. 2004, ApJ, 608, 663
Kennicutt, R. C. 1998, ApJ, 498, 541
Klypin, A., Kravtsov, A. V., Valenzuela, O., & Prada, F. 1999, ApJ, 522, 82
Kravtsov, A. V., Gnedin, O. Y., & Klypin, A. A. 2004, ApJ, 609, 482
Kroupa, P., Tout, C. A., & Gilmore, G. 1993, MNRAS, 262, 545
Lanfranchi, G. A., & Matteucci, F. 2003, MNRAS, 345, 71
———. 2004, MNRAS, 351, 1338
Lanfranchi, G. A., Matteucci, F., & Cescutti, G. 2006, MNRAS, 365, 477
Majewski, S. R., Patterson, R. J., Dinescu, D. I., Johnson, W. Y., Ostheimer, J. C., Kunkel, W. E., & Palma, C. 2000, in Proc. Liege Int. Astrophys. Colloq. 35, The Galactic Halo: From Globular Cluster to Field Stars, ed. A. Noels et al. (Belgium: Inst. d'Astrophys.), 619
Marcolini, A., Brighenti, F., & D'Ercole, A. 2003, MNRAS, 345, 1329
———. 2004, MNRAS, 352, 363
Marcolini, A., D'Ercole, A., & Brighenti, F. 2006, MNRAS, submitted (astro-ph /0602386)
Martin, C. L., Kobulnicky, H. A., & Heckman, T. M. 2002, ApJ, 574, 663
Mashchenko, S., Couchman, H. M. P., & Sills, A. 2005, ApJ, 624, 726
Mateo, M. L. 1998, ARA&A, 36, 435
Matteucci, F., & Greggio, L. 1986, A&A, 154, 279
Matteucci, F., & Recchi, S. 2001, ApJ, 558, 351
Mayer, L., Mastropietro, C., Wadsley, J., Stadel, J., & Moore, B. 2005, MNRAS, submitted (astro-ph/0504277)
Read, J. I., Wilkinson, M. I., Evans, N. W., Gilmore, G., & Kleyna, J. T. 2006, MNRAS, 367, 387
Recchi, S., Hensler, G., Angeretti, L., & Matteucci, F. 2006, A&A, 445, 875
Recchi, S., Matteucci, F., D'Ercole, A., & Tosi, M. 2004, A&A, 426, 37
Ricotti, M., & Gnedin, N. Y. 2005, ApJ, 629, 259
Robertson, B., Bullock, J. S., Font, A. S., Johnston, K. V., & Hernquist, L. 2005, ApJ, 632, 872
Schaller, G., Schaerer, D., Meynet, G., & Maeder, A. 1992, A&AS, 96, 269
Shetrone, M., Venn, K. A., Tolstoy, E., Primas, F., Hill, V., & Kaufer, A. 2003, AJ, 125, 684
Shu, C.-G., Mo, H.-J., & Mao, S.-D. 2005, Chinese J. Astron. Astrophys., 5, 327
Silk, J. 2003, MNRAS, 343, 249
Smith, V. V., Suntzeff, N. B., Cunha, K., Gallino, R., Busso, M., Lambert, D. L., & Straniero, O. 2000, AJ, 119, 1239
Sumiyoshi, K., Terasawa, M., Mathews, G. J., Kajino, T., Yamada, S., & Suzuki, H. 2001, ApJ, 562, 880
Thielemann, F.-K., Nomoto, K., & Yokoi, K. 1986, A&A, 158, 17
Tian, K. P., van Leeuwen, F., Zhao, J. L., & Su, C. G. 1996, A&AS, 118, 503
Timmes, F. X., Woosley, S. E., & Weaver, T. A. 1995, ApJS, 98, 617
Travaglio, C., Galli, D., Gallino, R., Busso, M., Ferrini, F., & Straniero, O. 1999, ApJ, 521, 691
Travaglio, C., Gallino, R., Arnone, E., Cowan, J., Jordan, F., & Sneden, C. 2004, ApJ, 601, 864
Travaglio, C., Gallino, R., Busso, M., & Gratton, R. 2001, ApJ, 549, 346
Tsujimoto, T., Shigeyama, T., & Yoshii, Y. 2000, ApJ, 531, L33
Venn, K. A., Irwin, M., Shetrone, M. D., Tout, C. A., Hill, V., & Tolstoy, E. 2004, AJ, 128, 1177
Wanajo, S., Tamamura, M., Itoh, N., Nomoto, K., Ishimaru, Y., Beers, T. C., & Nozawa, S. 2003, ApJ, 593, 968
Woosley, S. E., & Weaver, T. A. 1995, ApJS, 101, 181